

## Lensing clusters of galaxies in the SDSS-III \*

Zhong-Lue Wen, Jin-Lin Han and Yun-Ying Jiang

National Astronomical Observatories, Chinese Academy of Sciences, Beijing 100012, China;  
[zhonglue@nao.cas.cn](mailto:zhonglue@nao.cas.cn)

Received 2011 May 27; accepted 2011 June 27

**Abstract** We identify new strong lensing clusters of galaxies from the Sloan Digital Sky Survey III (SDSS DR8) by visually inspecting color images of a large sample of clusters of galaxies. We find 68 new clusters showing giant arcs in addition to 30 known lensing systems. Among 68 cases, 13 clusters are “*almost certain*” lensing systems with tangential giant arcs, 22 clusters are “*probable*” and 31 clusters are “*possible*” lensing systems. We also find two exotic systems with blue rings. The giant arcs have angular separations of  $2.0'' - 25.7''$  from the bright central galaxies. We note that the rich clusters are more likely to be lensing systems and the separations between the arcs and the central galaxies increase with cluster richness.

**Key words:** galaxies: clusters: general — gravitational lensing

### 1 INTRODUCTION

Gravitational lensing is the phenomenon of light deflection by gravitational fields. Strong lensing occurs when a lens and a background source lie very close along the line of sight. Thus, it is a relatively rare phenomenon in the universe. As the largest bound systems in the universe, galaxy clusters are the most powerful gravitational lenses to magnify background sources. They distort background galaxies into giant arcs or multiple images. Strong lensing by galaxy clusters can be used to study the faint background galaxies at high redshift (e.g. Miralda-Escude & Fort 1993; Metcalfe et al. 2003) and to directly measure cosmological parameters (e.g., Bolton & Burles 2003). The statistics of giant lensing arcs help to understand the structure formation and cosmology paradigm (e.g. Wu & Mao 1996; Bartelmann et al. 1998; Li et al. 2005). The strong lensing by galaxies or galaxy clusters has been proposed to test other gravity theories (e.g., TeVeS theory, Chen & Zhao 2006). Moreover, strong lensing is a unique method to examine the model of mass distribution in halos (e.g. Takahashi & Chiba 2001; Shu et al. 2008; Li & Chen 2009; Chen & McGaugh 2010). The determined mass from lensing features is model independent and therefore can be used to calibrate the mass estimates derived from X-ray observations (Wu 2000).

Generally, lensed arcs are very faint. They can be found from imaging surveys and confirmed by later spectroscopic observations. Searches for arcs are usually performed with high quality image data. Up to now, less than two hundred strong lensing clusters have been discovered by visual inspection of images (e.g. Gladders et al. 2003; Sand et al. 2005) or by automated search of the images (e.g., Cabanac et al. 2007; Limousin et al. 2009). Systematic searches for lensing systems have been made for massive clusters due to their powerful magnification. From 38 X-ray luminous

\* Supported by the National Natural Science Foundation of China.

clusters, Luppino et al. (1999) found eight clusters with giant arcs, two clusters with arclets and six lensing candidates. Using the *HST* WFC2 data, Sand et al. (2005) found 104 giant arcs from 54 rich clusters. Hennawi et al. (2008) found 16 new lensing clusters with giant arcs, with 12 likely lensing clusters and 9 possible candidates based on 240 rich clusters from the Sloan Digital Sky Survey (SDSS) and follow-up deep imaging observations.

The SDSS has provided relatively shallow images in five broad bands ( $u, g, r, i$  and  $z$ ) with a detection limit of  $r = 22.5$  and a seeing of  $1.43''$  (Stoughton et al. 2002). Because it covers one-fifth of the sky, tens of lensing systems have been recently discovered. Some lensing systems were serendipitously discovered, e.g., the “8 O’clock arc” (Allam et al. 2007) and the Hall’s arc (Estrada et al. 2007). More lens systems, e.g., the “Cosmic horseshoe” and the “Cheshire Cat” (Belokurov et al. 2007, 2009), were discovered in the systematic searches. The “CASSOWARY”<sup>1</sup> project searches for wide separation ( $> 1.5''$ ) gravitational lensing systems around massive elliptical galaxies in the SDSS with follow-up spectroscopic observations (Pettini et al. 2010; Christensen et al. 2010). The “Sloan Bright Arcs Survey” is a similar project to search for lensing candidates around massive galaxies and make spectroscopic confirmation (Diehl et al. 2009; Kubo et al. 2009). By visually inspecting color images of 39 668 clusters, Wen et al. (2009b) preformed a search for giant arcs and found four new lensing systems and another nine lensing candidates. Most of them have been spectroscopically confirmed later by other observers (see Table 1). Some arcs in the SDSS images, e.g., the “8 O’clock arc” and the “Cosmic horseshoe,” are lensed by individual galaxies, but more giant arcs are generated by clusters or groups of galaxies.

In this paper, we report the discovery of 68 lensing cluster candidates from a large galaxy cluster sample identified from the SDSS-III.

## 2 NEW LENSING CLUSTERS IN THE SDSS-III

Visually inspecting images is an efficient method to search for lensed arcs (e.g., Luppino et al. 1999; Sand et al. 2005). Following the procedure of Wen et al. (2009b), we first identify a large sample of galaxy clusters and then visually inspect their color images for lensing systems.

Using photometric redshifts of galaxies, Wen et al. (2009a) identified 39 668 clusters from  $\sim 8\,400 \text{ deg}^2$  of the SDSS DR6. We now improve the method to identify clusters of galaxies from  $\sim 14\,000 \text{ deg}^2$  of the SDSS-III (DR8, Aihara et al. 2011). A cluster is identified when the richness reaches  $R = 12$  within a radius  $r_{200}$  and a photometric redshift gap between  $z \pm 0.04(1+z)$ . Here  $r_{200}$  is the radius within which the mean density is 200 times the critical density of the universe. The cluster richness,  $R$ , is defined to be the average number of  $L^*$  galaxies, i.e.,  $R = \sum L_r / L^*$ , where  $\sum L_r$  is the  $r$ -band total luminosity of cluster galaxies after the background subtraction.  $L^*$  is the characteristic luminosity in the Schechter luminosity function (Blanton et al. 2003). From the SDSS-III data, we now identify about 130 000 clusters in the redshift range of  $0.05 < z < 0.8$  (Wen et al. 2011, in preparation). By inspecting color images on the SDSS web page<sup>2</sup>, we find 68 new clusters with giant arcs in addition to 30 known lensing clusters. They are listed in Table 1. Among them, 13 clusters are *almost certain* lensing systems (see Fig. 1) which show tangential giant arcs or multiple tangential giant arcs with respect to the bright central galaxies with a separation of  $S = 2.0'' - 18.5''$ . The faint but clear arcs usually have blue colors compared with the bright central galaxies. Remarkably, SDSS J005848.9–072156 shows the giant arc almost forming a half circle with a radius of  $S = 14.4''$ . In a  $\Lambda$ CDM cosmology ( $H_0 = 72 \text{ km s}^{-1} \text{ Mpc}^{-1}$ ,  $\Omega_m = 0.3$  and  $\Omega_\Lambda = 0.7$ , hereafter), we estimate the mass within this radius by Wu (2000),

$$M(< S) = \frac{c^2 S^2}{4G} \frac{D_l D_s}{D_{ls}}, \quad (1)$$

<sup>1</sup> <http://www.ast.cam.ac.uk/ioa/research/cassowary>

<sup>2</sup> <http://skyserver.sdss3.org/dr8/en/tools/chart/list.asp>

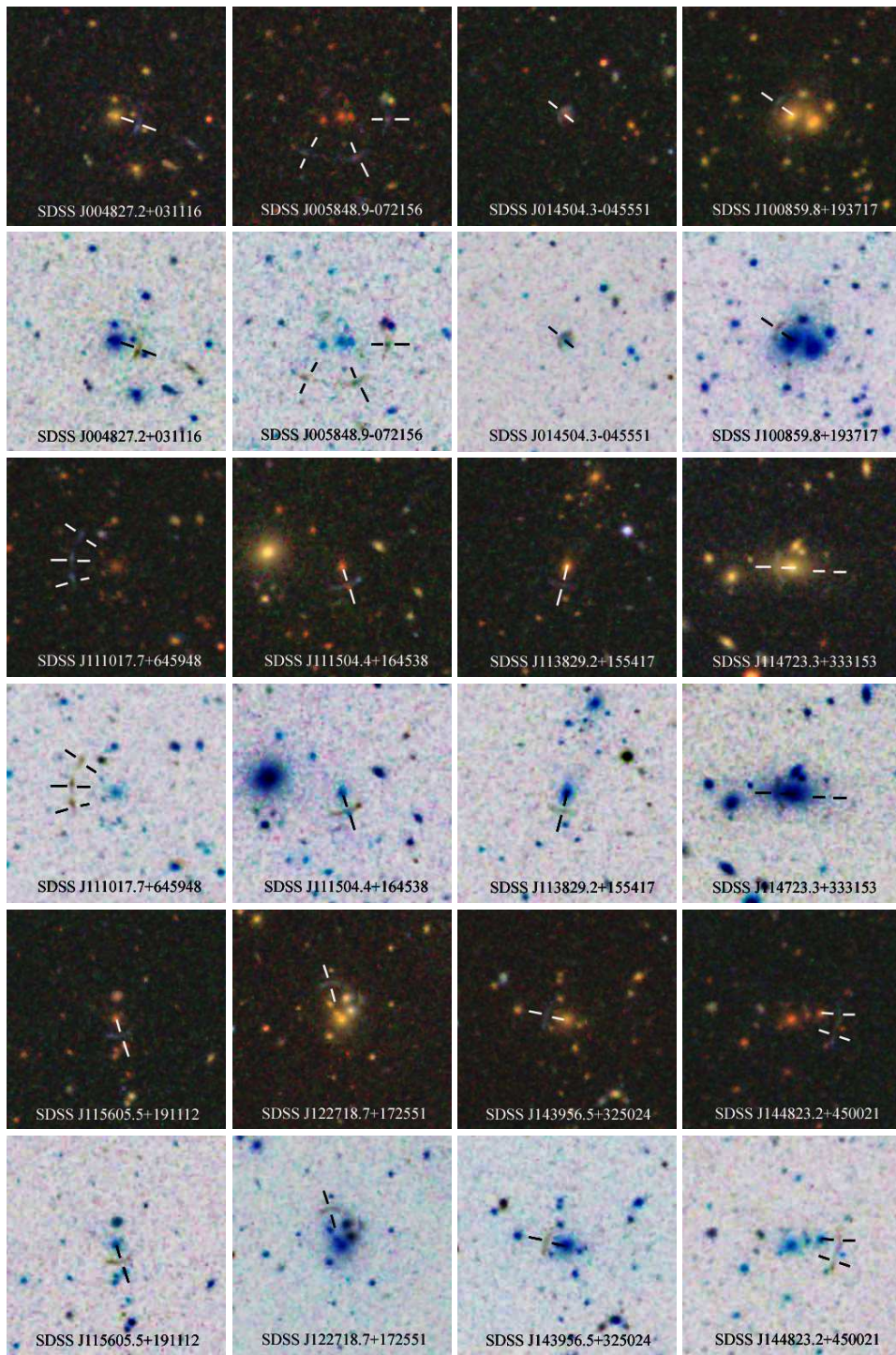
**Table 1** Strong Lensing Clusters in the SDSS-III

Cluster name (1)	Cluster $z$ (2)	Richness (3)	$S$ ( $''$ ) (4)	$r$ (mag) (5)	$g - r$ (mag) (6)	Reference, Notes (7)
SDSS J002240.9+143110	0.380	18.96	3.3	21.37 $\pm$ 0.08	0.19 $\pm$ 0.11	[1]
SDSS J014656.0-092952	0.448	66.11	9.2	21.75 $\pm$ 0.12	3.00 $\pm$ 0.74	[2, 3]
SDSS J023953.1-013455	0.375	169.43	25.7	22.38 $\pm$ 0.18	2.04 $\pm$ 0.55	[4]
SDSS J024803.4-033145	0.188	108.18	16.4	22.67 $\pm$ 0.21	0.20 $\pm$ 0.26	[5]
SDSS J082728.4+223245	0.335	108.26	2.2	21.12 $\pm$ 0.06	-0.20 $\pm$ 0.08	[6]
SDSS J090002.6+223404	0.489	19.37	7.0	21.08 $\pm$ 0.06	-0.11 $\pm$ 0.08	[7, 8]
SDSS J095240.2+343446	0.354	46.10	6.9	22.09 $\pm$ 0.14	0.92 $\pm$ 0.26	[9]
SDSS J095739.2+050931	0.429	16.06	8.0	19.90 $\pm$ 0.07	0.19 $\pm$ 0.09	[7, 9, 10]
SDSS J103843.6+484917	0.426	19.44	7.8	22.06 $\pm$ 0.14	0.09 $\pm$ 0.17	[10, 11, 12]
SDSS J111310.6+235639	0.336	80.47	11.5	23.25 $\pm$ 0.26	0.07 $\pm$ 0.32	[7, 12]
SDSS J113313.2+500840	0.370	18.78	10.4	23.07 $\pm$ 0.24	0.36 $\pm$ 0.33	[5]
SDSS J113740.1+493635	0.448	15.43	3.7	20.35 $\pm$ 0.04	0.05 $\pm$ 0.05	[7, 12]
SDSS J115200.2+331342	0.357	63.85	7.9	23.61 $\pm$ 0.51	-0.56 $\pm$ 0.55	[10]
SDSS J120602.1+514229	0.422	18.96	3.8	19.93 $\pm$ 0.06	0.39 $\pm$ 0.08	[13]
SDSS J120735.9+525459	0.282	24.77	9.4	22.54 $\pm$ 0.18	-0.06 $\pm$ 0.21	[7, 9]
SDSS J120923.7+264046	0.559	110.76	10.6	22.98 $\pm$ 0.30	-0.11 $\pm$ 0.35	[10, 14]
SDSS J122651.7+215225	0.433	117.13	10.9	22.28 $\pm$ 0.18	0.26 $\pm$ 0.24	[7, 10]
SDSS J124032.3+450902	0.251	19.40	3.8	20.16 $\pm$ 0.04	-0.27 $\pm$ 0.04	[11]
SDSS J131811.5+394226	0.475	26.81	8.5	22.16 $\pm$ 0.15	0.33 $\pm$ 0.21	[7, 9]
SDSS J134332.9+415503	0.418	37.84	12.7	22.31 $\pm$ 0.19	0.20 $\pm$ 0.24	[7, 8, 10]
SDSS J141912.2+532611	0.638	22.80	10.0	21.85 $\pm$ 0.14	0.26 $\pm$ 0.17	[15]
SDSS J151118.7+471340	0.451	31.15	5.4	23.26 $\pm$ 1.18	-2.56 $\pm$ 1.18	[12]
SDSS J152745.8+065233	0.400	92.84	17.7	21.65 $\pm$ 0.16	-0.02 $\pm$ 0.17	[3, 10, 16]
SDSS J153713.2+655621	0.251	32.99	8.1	22.64 $\pm$ 0.24	0.33 $\pm$ 0.31	[9]
SDSS J162132.4+060719	0.361	49.20	16.1	21.51 $\pm$ 0.10	0.96 $\pm$ 0.20	[7, 10]
SDSS J172336.2+341158	0.442	34.78	4.7	20.56 $\pm$ 0.04	-0.21 $\pm$ 0.05	[7, 9]
SDSS J211119.3-011423	0.638	22.70	10.9	21.23 $\pm$ 0.17	0.04 $\pm$ 0.22	[3]
SDSS J223831.3+131955	0.413	38.35	9.3	22.61 $\pm$ 0.16	0.60 $\pm$ 0.27	[7, 10]
SDSS J223933.1-042917	0.553	23.10	3.4	22.34 $\pm$ 0.20	-0.16 $\pm$ 0.23	[17]
SDSS J224712.3-020537	0.329	88.14	9.0	22.44 $\pm$ 0.19	0.66 $\pm$ 0.30	[5]
SDSS J004827.2+031116	0.337	13.64	8.0	22.04 $\pm$ 0.14	-0.25 $\pm$ 0.16	almost certain
SDSS J005848.9-072156	0.619	33.35	14.4	20.03 $\pm$ 0.11	0.14 $\pm$ 0.14	almost certain
SDSS J014504.3-045551	0.604	16.64	2.0	21.83 $\pm$ 0.14	0.08 $\pm$ 0.17	almost certain
SDSS J100859.8+193717	0.306	43.85	6.1	22.99 $\pm$ 0.28	0.51 $\pm$ 0.44	almost certain*
SDSS J111017.7+645948	0.601	29.55	14.9	21.42 $\pm$ 0.11	0.40 $\pm$ 0.15	almost certain
SDSS J111504.4+164538	0.588	15.35	6.9	21.89 $\pm$ 0.12	0.15 $\pm$ 0.15	almost certain
SDSS J113829.2+155417	0.450	27.84	6.8	23.35 $\pm$ 0.38	-0.32 $\pm$ 0.43	almost certain
SDSS J114723.3+333153	0.212	34.47	5.3	23.12 $\pm$ 0.30	-0.09 $\pm$ 0.35	almost certain
SDSS J115605.5+191112	0.516	13.05	5.5	22.76 $\pm$ 0.23	-0.13 $\pm$ 0.27	almost certain
SDSS J122718.7+172551	0.308	14.73	11.8	24.42 $\pm$ 0.58	-0.61 $\pm$ 0.65	almost certain*
SDSS J143956.5+325024	0.418	56.22	7.7	22.94 $\pm$ 0.23	-0.03 $\pm$ 0.28	almost certain
SDSS J144823.2+450021	0.554	36.75	15.3	22.66 $\pm$ 0.18	-0.14 $\pm$ 0.22	almost certain
SDSS J230017.3+221329	0.444	46.64	18.5	21.46 $\pm$ 0.14	0.41 $\pm$ 0.19	almost certain
SDSS J001331.9+351220	0.228	25.94	10.0	20.99 $\pm$ 0.10	0.25 $\pm$ 0.13	probable
SDSS J002556.3+362439	0.322	19.55	9.3	22.41 $\pm$ 0.18	1.59 $\pm$ 0.43	probable
SDSS J003237.3+073649	0.481	24.21	6.9	20.94 $\pm$ 0.07	0.07 $\pm$ 0.09	probable
SDSS J010049.2+181827	0.650	29.07	5.5	22.55 $\pm$ 0.22	0.52 $\pm$ 0.30	probable
SDSS J014350.1+160739	0.452	20.13	2.8	22.15 $\pm$ 0.18	-0.38 $\pm$ 0.20	probable
SDSS J090122.4+181432	0.346	21.01	6.5	22.35 $\pm$ 0.16	0.92 $\pm$ 0.27	probable
SDSS J100202.5+602026	0.573	46.01	14.8	22.32 $\pm$ 0.20	1.54 $\pm$ 0.48	probable
SDSS J100226.8+203101	0.321	135.69	14.1	—	—	probable
SDSS J104044.6+330520	0.615	41.43	7.9	22.52 $\pm$ 0.16	0.03 $\pm$ 0.20	probable
SDSS J104601.1+104852	0.258	14.06	5.8	21.72 $\pm$ 0.14	0.07 $\pm$ 0.17	probable
SDSS J115120.6+645530	0.561	36.75	17.2	22.17 $\pm$ 0.14	1.05 $\pm$ 0.28	probable

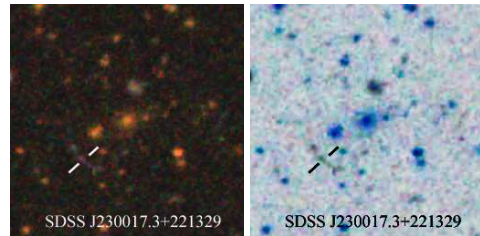
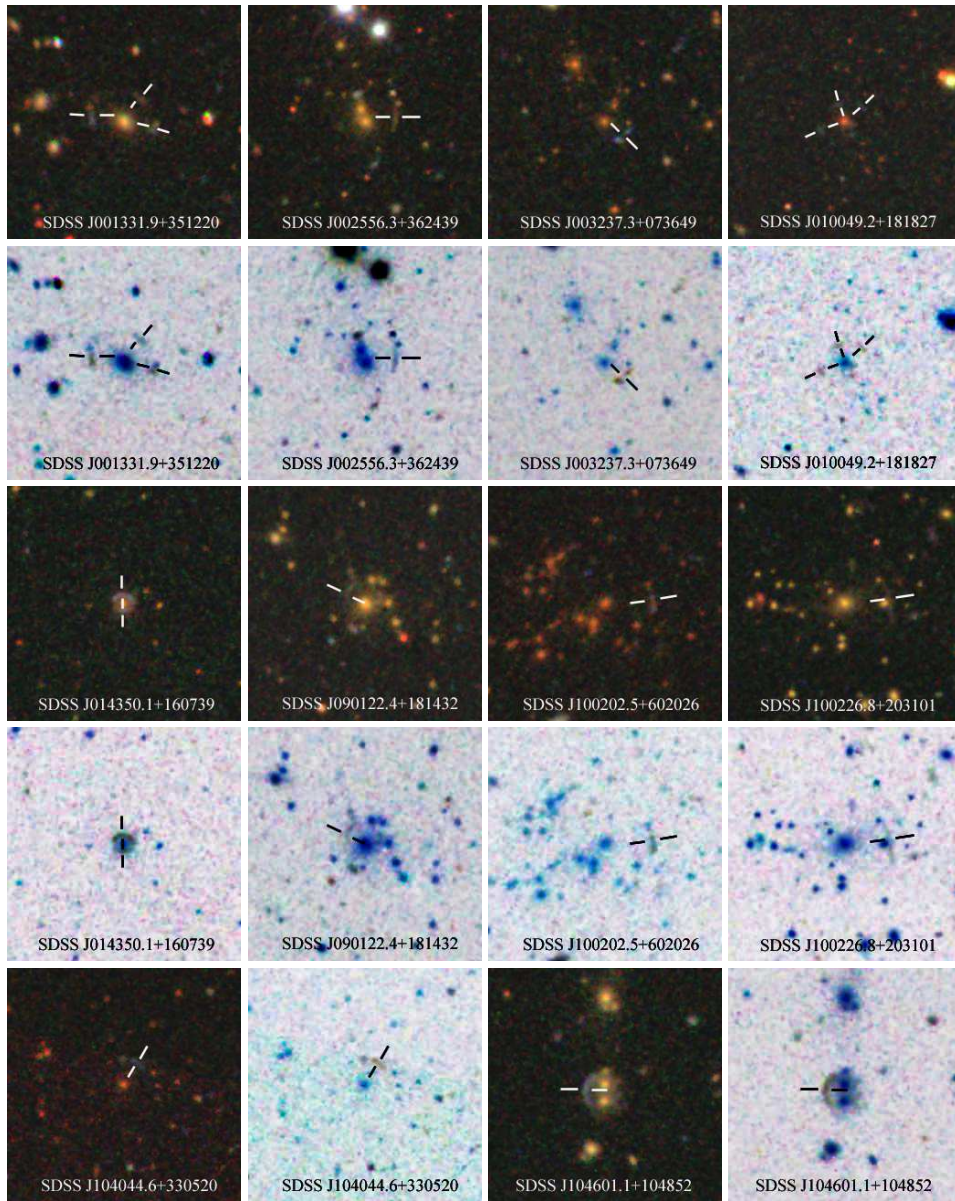
**Table 1** — *Continued*

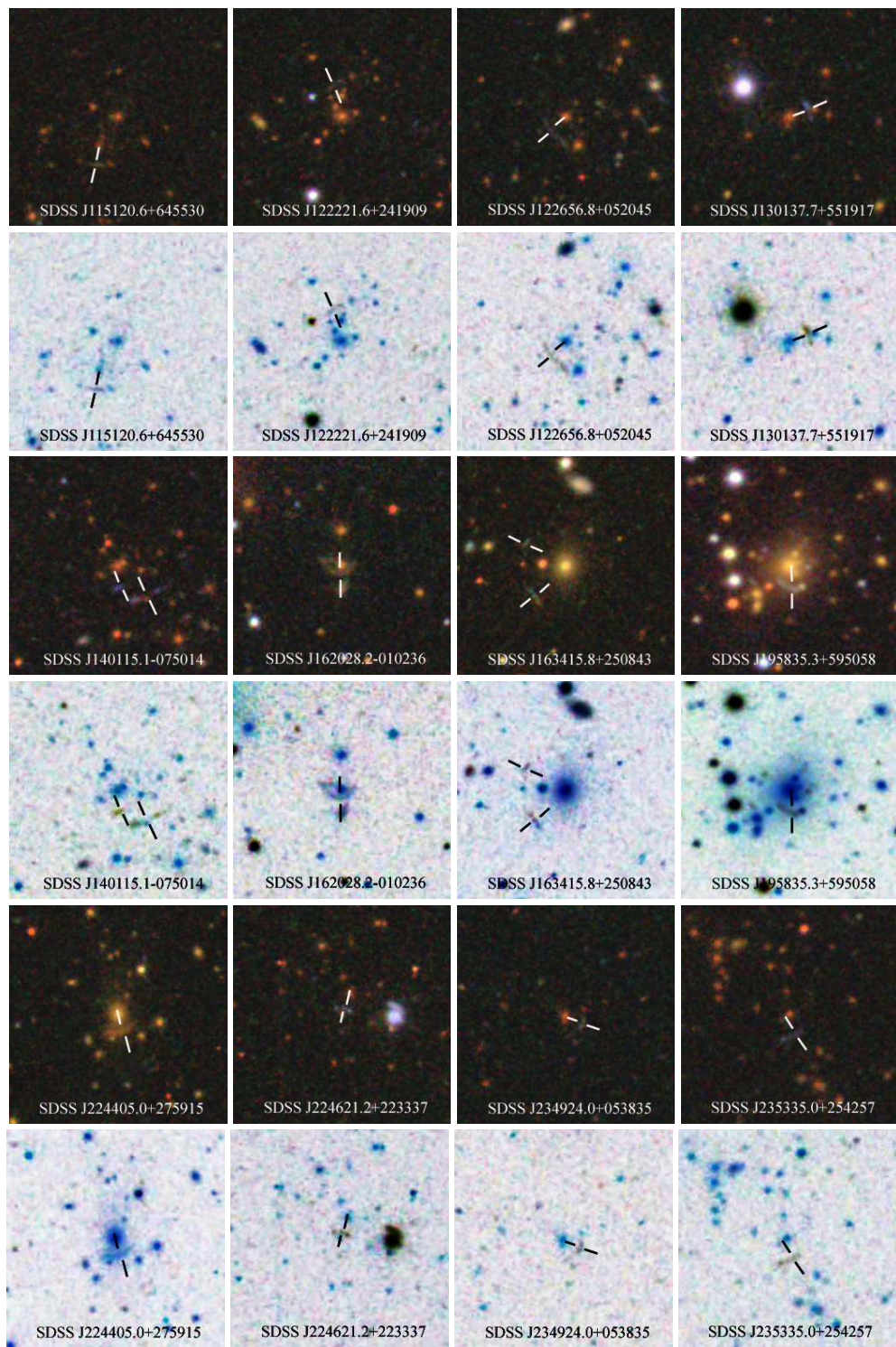
Cluster name	Cluster $z$	Richness	$S$ ( $\text{''}$ )	$r$ (mag)	$g - r$ (mag)	Reference, Notes
(1)	(2)	(3)	(4)	(5)	(6)	(7)
SDSS J122221.6+241909	0.501	52.21	11.7	$22.88 \pm 0.23$	$0.21 \pm 0.31$	probable
SDSS J122656.8+052045	0.504	25.84	8.6	$22.04 \pm 0.16$	$0.48 \pm 0.24$	probable
SDSS J130137.7+551917	0.606	24.11	6.8	$21.37 \pm 0.09$	$-0.16 \pm 0.10$	probable
SDSS J140115.1–075014	0.508	96.27	12.4	$21.23 \pm 0.09$	$0.22 \pm 0.12$	probable
SDSS J162028.2–010236	0.370	13.68	3.4	$22.03 \pm 0.14$	$1.69 \pm 0.43$	probable
SDSS J163415.8+250843	0.221	20.41	14.2	$21.02 \pm 0.09$	$0.84 \pm 0.15$	probable
SDSS J195835.3+595058	0.231	74.24	7.9	$20.37 \pm 0.04$	$0.50 \pm 0.07$	probable
SDSS J224405.0+275915	0.352	54.52	6.4	$22.53 \pm 0.21$	$1.29 \pm 0.42$	probable
SDSS J224621.2+223337	0.571	12.72	2.7	$21.88 \pm 0.10$	$0.37 \pm 0.13$	probable
SDSS J234924.0+053835	0.692	54.02	6.4	$21.53 \pm 0.11$	$0.66 \pm 0.18$	probable
SDSS J235335.0+254257	0.521	12.70	8.5	$21.48 \pm 0.12$	$0.30 \pm 0.17$	probable
SDSS J002547.5+285329	0.342	19.47	7.2	$20.77 \pm 0.05$	$0.03 \pm 0.06$	possible
SDSS J002824.1+224802	0.449	32.12	18.8	$20.48 \pm 0.07$	$1.07 \pm 0.13$	possible
SDSS J005403.9+185504	0.477	19.27	7.5	$19.74 \pm 0.18$	$4.58 \pm 6.73$	possible
SDSS J005529.8+074114	0.366	22.17	11.4	$20.79 \pm 0.10$	$2.48 \pm 0.58$	possible
SDSS J010842.0+062443	0.564	35.23	3.1	$20.85 \pm 0.07$	$-0.02 \pm 0.08$	possible
SDSS J020638.9+044803	0.268	38.72	5.4	$20.25 \pm 0.08$	$0.31 \pm 0.10$	possible
SDSS J080731.5+441048	0.449	15.54	2.9	$22.83 \pm 0.26$	$0.29 \pm 0.36$	possible
SDSS J082854.3+103408	0.312	32.38	12.8	$21.04 \pm 0.06$	$0.51 \pm 0.09$	possible
SDSS J084647.5+044605	0.242	38.94	4.2	$21.91 \pm 0.14$	$-0.38 \pm 0.15$	possible
SDSS J085428.7+100814	0.298	28.59	4.5	$22.30 \pm 0.17$	$0.19 \pm 0.23$	possible
SDSS J105559.4+155514	0.284	16.03	6.1	$21.74 \pm 0.15$	$0.27 \pm 0.19$	possible
SDSS J110934.8+142953	0.476	22.20	10.2	$22.39 \pm 0.15$	$1.12 \pm 0.27$	possible
SDSS J112229.5+212416	0.380	12.00	4.3	$21.35 \pm 0.07$	$0.65 \pm 0.12$	possible
SDSS J113912.9+165435	0.579	28.89	20.9	$20.33 \pm 0.05$	$0.65 \pm 0.08$	possible
SDSS J120453.5+135753	0.533	20.22	3.2	$22.98 \pm 0.27$	$-0.08 \pm 0.33$	possible
SDSS J123736.2+553343	0.410	24.66	4.5	$19.96 \pm 0.03$	$-0.04 \pm 0.04$	possible, 7*
SDSS J133145.3+513431	0.283	33.34	3.4	$23.37 \pm 0.29$	$-0.12 \pm 0.35$	possible
SDSS J133314.4+184637	0.315	15.44	5.3	$22.68 \pm 0.18$	$1.27 \pm 0.39$	possible
SDSS J140110.4+565420	0.493	32.84	3.8	$21.50 \pm 0.08$	$0.45 \pm 0.12$	possible
SDSS J142040.9+400454	0.634	23.26	14.6	$20.46 \pm 0.07$	$0.36 \pm 0.09$	possible
SDSS J144355.0+585302	0.156	21.55	7.3	$23.72 \pm 0.51$	$-1.06 \pm 0.53$	possible
SDSS J145836.3–002400	0.570	25.02	3.8	$21.69 \pm 0.11$	$1.00 \pm 0.21$	possible
SDSS J150236.6+292053	0.554	22.88	2.2	$21.46 \pm 0.08$	$0.72 \pm 0.12$	possible
SDSS J150510.8+172042	0.511	28.24	4.0	$22.54 \pm 0.17$	$2.11 \pm 0.51$	possible
SDSS J172535.3+654153	0.519	20.40	6.3	$22.69 \pm 0.24$	$0.13 \pm 0.31$	possible
SDSS J212326.0+015312	0.551	15.19	3.6	$22.05 \pm 0.12$	$0.75 \pm 0.20$	possible
SDSS J213340.5–050055	0.316	55.44	9.0	$20.46 \pm 0.05$	$0.12 \pm 0.06$	possible
SDSS J222208.6+274535	0.488	37.59	10.8	$21.66 \pm 0.11$	$0.25 \pm 0.14$	possible
SDSS J224859.0+014711	0.372	37.23	8.8	$22.06 \pm 0.16$	$0.41 \pm 0.24$	possible
SDSS J234028.5+294747	0.496	12.05	2.7	$22.29 \pm 0.20$	$-0.39 \pm 0.22$	possible
SDSS J234744.1+051324	0.491	24.75	2.4	$21.83 \pm 0.12$	$1.51 \pm 0.34$	possible
SDSS J113843.7+120802	0.177	13.66	9.2	$20.80 \pm 0.06$	$0.22 \pm 0.09$	exotic ring
SDSS J155719.4+270416	0.068	12.00	16.8	$22.21 \pm 0.14$	$1.03 \pm 0.25$	exotic ring

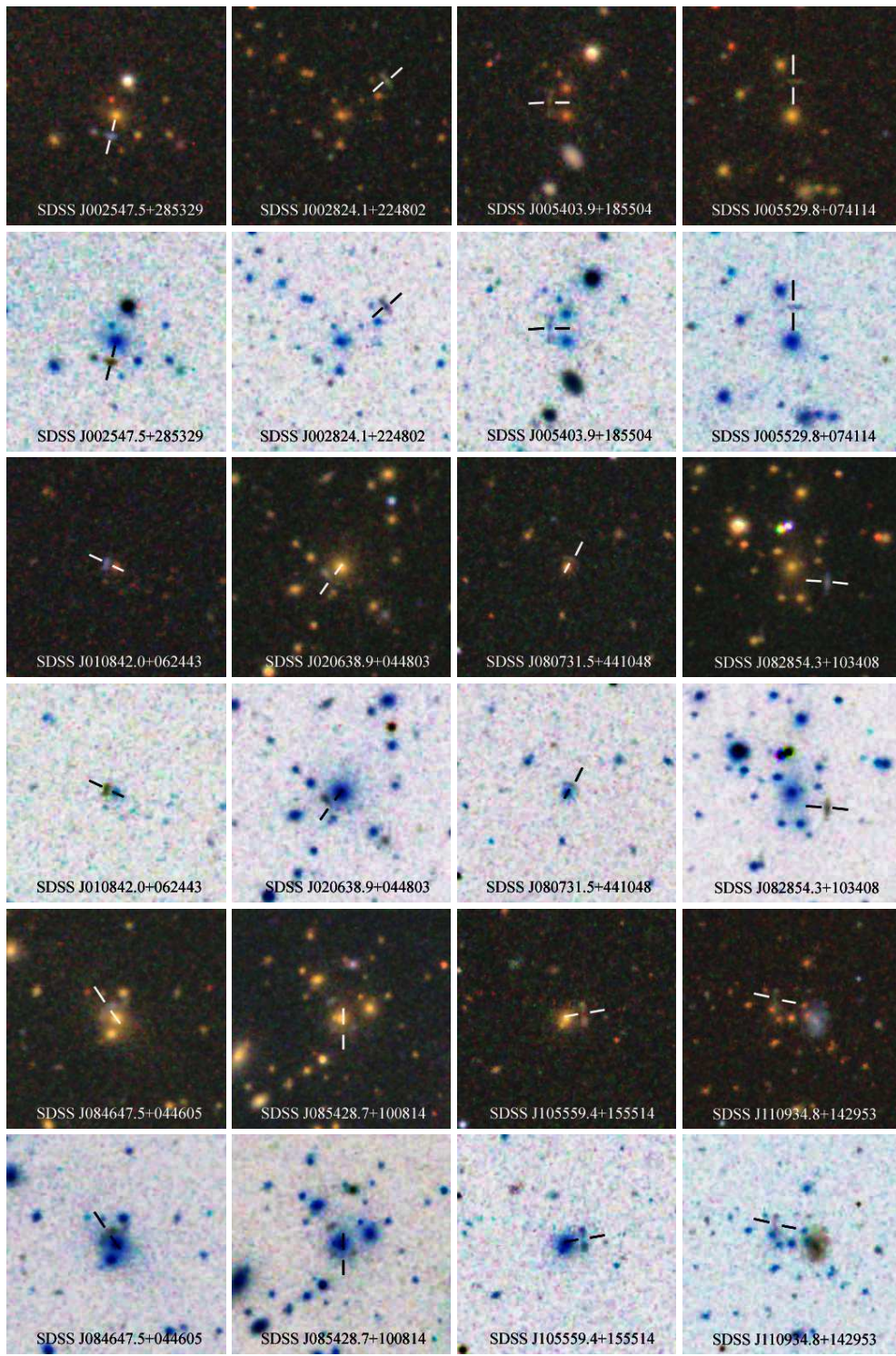
Notes: Here we list the name, redshift and richness of galaxy clusters in Cols. (1), (2) and (3), respectively. The angular separation ( $S$ ) between the arc and the central galaxy is listed in Col. (4), the  $r$ -band magnitude and color ( $g - r$ ) of the brightest part of arc are given in Cols. (5) and (6), respectively. References and notes on the lensing systems are given in Col. (7). References are: [1] Allam et al. (2007); [2] Estrada et al. (2007); [3] Hennawi et al. (2008); [4] Hammer & Rigaut (1989); [5] Sand et al. (2005); [6] Shin et al. (2008); [7] Wen et al. (2009b); [8] Diehl et al. (2009); [9] Kubo et al. (2010); [10] Bayliss et al. (2011); [11] Belokurov et al. (2009); [12] Kubo et al. (2009); [13] Lin et al. (2009); [14] Ofek et al. (2008); [15] Gladders et al. (2003); [16] Koester et al. (2010); [17] Swinbank et al. (2006). \*: CASSOWARY candidates, see <http://www.ast.cam.ac.uk/research/cassowary>.



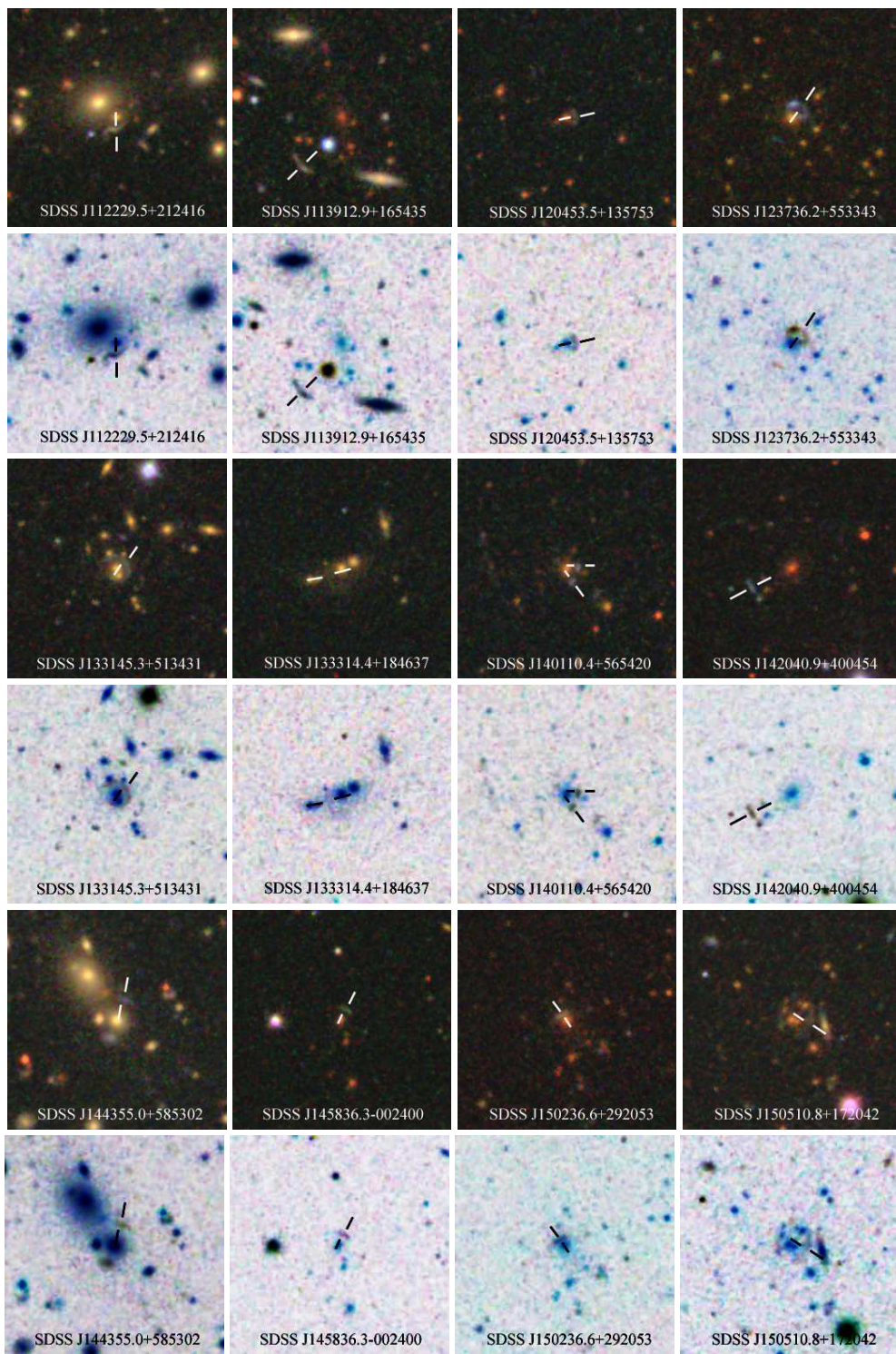
**Fig. 1** SDSS composite color images (*g*, *r* and *i*) of 13 clusters (one in the next page) with a field of view of  $1.2' \times 1.2'$ . They are almost certain gravitational lensing systems. The negative images are also shown in the second rows to see the lensing features more clearly.

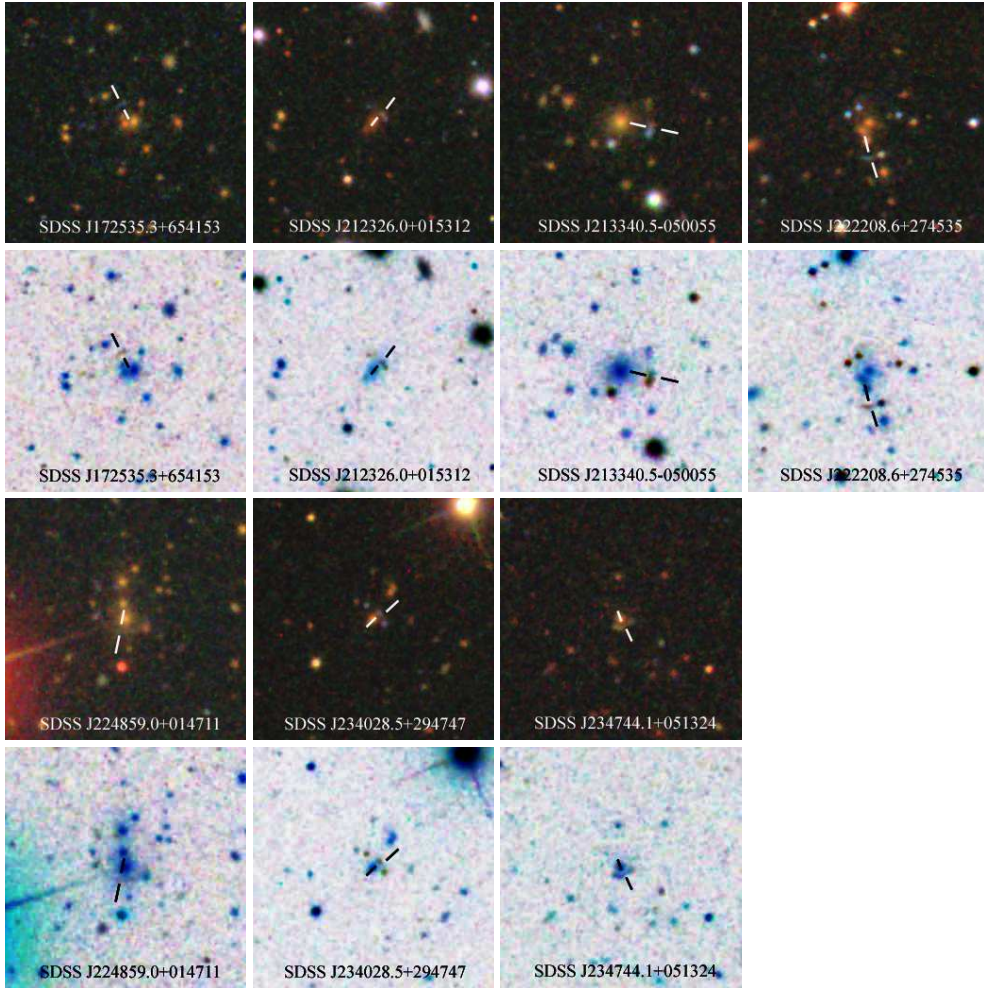
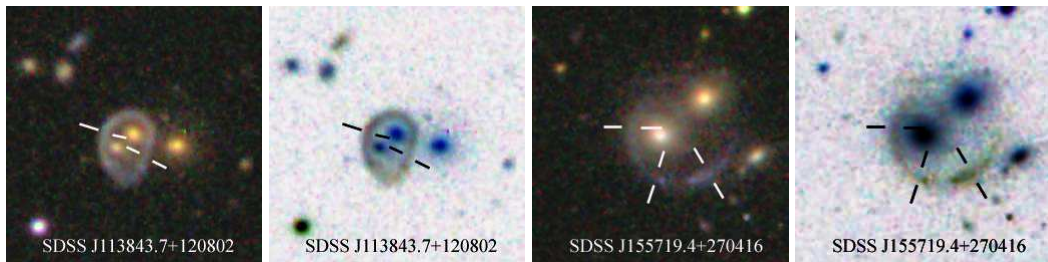
**Fig. 1 — Continued.****Fig. 2** Same as Fig. 1, but for 22 clusters (this and next page) which are *probable* lensing systems.

**Fig. 2 —** *Continued.*



**Fig. 3** Same as Fig. 1, but for 31 clusters (this and next two pages) which are *possible* lensing systems.

**Fig. 3 —** *Continued.*

**Fig. 3 —**Continued.**Fig. 4** Same as Fig. 1, but for two systems with *exotic* rings.

where  $D_s$  and  $D_l$  are the angular diameter distances of the source and lens from the observer and  $D_{ls}$  is the angular diameter distance of the source from the lens. We get the mass  $M(< S) = 1.1 \times 10^{14} M_\odot$  if the source has a redshift  $z_s = 1$ , or  $M(< S) = 0.61 \times 10^{14} M_\odot$  if  $z_s = 2$ .

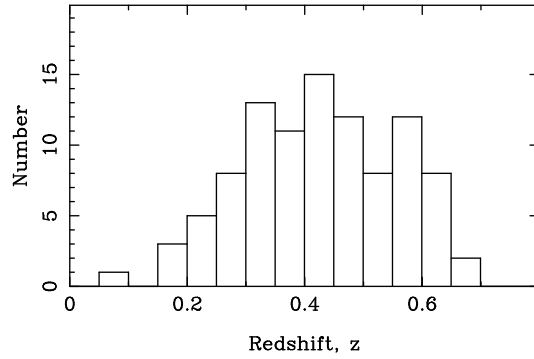


**Fig. 5** Redshift distribution of 98 lensing clusters identified from the SDSS-III images.

We find another 22 clusters which are *probable* lensing systems (see Fig. 2). They also show blue giant arcs, which are tangential to the bright central galaxies and are distinct in color from the reddish cluster galaxies. Generally, the arcs in these clusters are shorter than those in the “*almost certain*” systems. In some cases, we cannot exclude the possibility that the arcs are formed by galaxy interaction or the coincidental superposition of a few faint galaxies.

We also find another 31 clusters which are *possible* lensing systems (see Fig. 3). The arcs in these clusters also show blue colors but are shorter than those in the “*almost certain*” and “*probable*” lensing systems.

We find two clusters showing *exotic* rings (see Fig. 4) around two bright cluster member galaxies. In the cluster SDSS J113843.7+120802, the blue ring has a radius of  $7.5''$ . In this cluster, a brighter galaxy, SDSS J113842.8+120759, is located  $7.0''$  east of the ring, but the ring is not tangential to this galaxy. In the case of the cluster SDSS J155719.4+270416, a blue giant ring surrounds two member galaxies with redshifts  $z = 0.0678$  and  $0.0683$ . This giant ring has a radius of  $15''$ . If it is formed by strong lensing, the mass within the arc is  $7.8 \times 10^{12} M_{\odot}$  assuming the source redshift  $z_s = 2$ . If the giant arc is a star forming region, the system is an excellent example to study how galaxy merging triggers the star formation in their strange common halo.

Figure 5 shows the redshift distribution of 98 clusters with giant arcs which we identify from the SDSS-III images, 30 previously known lensing systems and 68 new. These clusters are distributed in the redshift range of  $\sim 0.1 < z < 0.7$  and have a redshift peak of  $z \sim 0.4$ .

### 3 DISTRIBUTION OF LENSING SYSTEMS

We notice that the lensed arcs preferably appear in the images of massive clusters. In Figure 6, we show the fraction of clusters as lensing systems against cluster richness,  $R$ . Clearly, the fraction,  $f$ , strongly depends on cluster richness. This is expected because richer clusters are more massive and have greater magnification factors. The fraction  $f \sim 10^{-4}$  is found for clusters with a richness of  $R \sim 10$  and it increases to  $\sim 10^{-3}$  for clusters with  $R \sim 30$  and  $\sim 10^{-2}$  for clusters with  $R \sim 100$ . The data are consistent with a power law

$$f = 10^{-6} R^2. \quad (2)$$

We also show the separation between the lensed arc and the central galaxy as a function of cluster richness,  $R$ . Although showing large scatters, richer lensing clusters tend to have larger separations. The data scatter may come from the variety of redshifts, locations of background galaxies and the cluster masses interior to the lensed arcs. To explain this general tendency, we draw three lines for the Einstein radius versus cluster richness with different parameters. The redshift of the lensing cluster

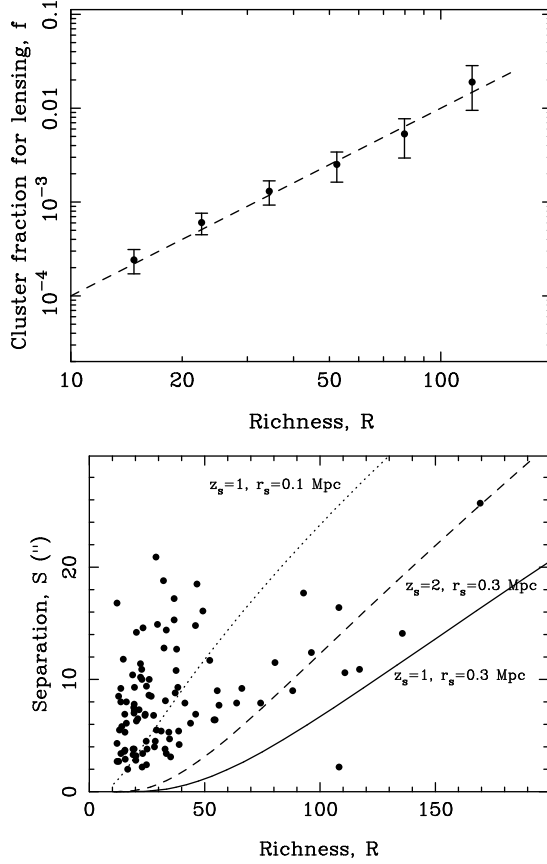


**Fig. 6** *Top panel:* the fraction of clusters as lensing systems against cluster richness. The dashed line is the power law of  $f = 10^{-6}R^2$ . *Bottom panel:* the separation between lensed arc and central galaxy against cluster richness. The lines are the Einstein radius against cluster richness for the cluster mass profiles and different redshifts of background sources (see text).

is set at  $z_l = 0.4$  (i.e., the peak of the redshift distribution in Fig. 5). The background source is placed at  $z_s = 1$  or  $z_s = 2$ . Considering the dark matter halo with a profile of Navarro et al. (1996)

$$\rho = \frac{\rho_s}{(r/r_s)(1+r/r_s)^2}, \quad (3)$$

where  $\rho_s$  and  $r_s$  are the characteristic density and radius, respectively, we can get the Einstein radius using Equation (1). The cluster mass,  $M_{200}$ , is related to the cluster richness,  $R$ , by (Wen et al. in preparation)

$$\log(M_{200}) = (-1.29 \pm 0.05) + (1.05 \pm 0.03) \log(R), \quad (4)$$

where  $M_{200}$  is the total mass within  $r_{200}$  in units of  $10^{14} M_\odot$ . For a cluster with a smaller  $r_s$ , the matter is more concentrated toward the cluster center, so that the cluster has a larger Einstein radius for the same  $z_l$  and  $z_s$ . We take  $r_s = 0.3 \text{ Mpc}$  or  $r_s = 0.1 \text{ Mpc}$  (Schmidt & Allen 2007) for calculation. As shown in Figure 6, for clusters with richness  $R > 50$ , the separations are consistent with the lensing systems with parameters between  $z_s = 1, r_s = 0.3 \text{ Mpc}$  and  $z_s = 1, r_s = 0.1$

Mpc. We notice that one rich cluster, SDSS J082728.4+223245 with a richness of  $R = 108.26$ , has an arc with a separation of  $2.2''$ , in which the arc is lensed by one of the member galaxies (Shin et al. 2008). For clusters with lower richesses of  $R < 50$ , the separations have large scatters and tend to be consistent with the calculation with a small  $r_s$ . This indicates that the lensing is obviously dominated by the bright central galaxy rather than the massive halo of a cluster.

#### 4 SUMMARY

By inspecting color images of a large sample of clusters of galaxies identified from the SDSS-III (DR8), we find 13 lensing clusters which are almost certain, together with 22 probable and 31 possible lensing clusters and two exotic systems. Together with 30 previously known lensing clusters, at least 43 lensing systems have been identified from the SDSS. The lensing clusters have a redshift in the range of  $\sim 0.1 < z < 0.7$ . The arcs in the cluster images have angular separations of  $2.0'' - 25.7''$  from the bright central galaxies and show bluer colors compared with the reddish cluster galaxies. We find that the fraction of clusters that act as lensing systems strongly depends on cluster richness. It increases from  $\sim 10^{-4}$  for clusters of richness  $R = 10$  to  $\sim 10^{-2}$  for clusters of  $R = 100$ . The separations between the arcs and the central galaxies tend to increase with cluster richness.

**Acknowledgements** The authors are supported by the National Natural Science Foundation of China (Grant Nos. 10821061, 10833003 and 11103032), Young Researcher Grant of National Astronomical Observatories, Chinese Academy of Sciences and the National Key Basic Research Science Foundation of China (2007CB815403). Funding for SDSS-III has been provided by the Alfred P. Sloan Foundation, the Participating Institutions, the National Science Foundation and the U.S. Department of Energy. The SDSS-III web site is <http://www.sdss3.org/>. SDSS-III is managed by the Astrophysical Research Consortium for the Participating Institutions of the SDSS-III Collaboration including the University of Arizona, the Brazilian Participation Group, Brookhaven National Laboratory, University of Cambridge, University of Florida, the French Participation Group, the German Participation Group, the Instituto de Astrofísica de Canarias, the Michigan State/Notre Dame/JINA Participation Group, Johns Hopkins University, Lawrence Berkeley National Laboratory, Max Planck Institute for Astrophysics, New Mexico State University, New York University, Ohio State University, Pennsylvania State University, University of Portsmouth, Princeton University, the Spanish Participation Group, University of Tokyo, University of Utah, Vanderbilt University, University of Virginia, University of Washington and Yale University.

#### References

- Aihara, H., Allende Prieto, C., An, D., et al. 2011, ApJS, 193, 29
- Allam, S. S., Tucker, D. L., Lin, H., et al. 2007, ApJ, 662, L51
- Bartelmann, M., Huss, A., Colberg, J. M., Jenkins, A., & Pearce, F. R. 1998, A&A, 330, 1
- Bayliss, M. B., Hennawi, J. F., Gladders, M. D., et al. 2011, ApJS, 193, 8
- Belokurov, V., Evans, N. W., Hewett, P. C., et al. 2009, MNRAS, 392, 104
- Belokurov, V., Evans, N. W., Moiseev, A., et al. 2007, ApJ, 671, L9
- Blanton, M. R., Hogg, D. W., Bahcall, N. A., et al. 2003, ApJ, 592, 819
- Bolton, A. S., & Burles, S. 2003, ApJ, 592, 17
- Cabanac, R. A., Alard, C., Dantel-Fort, M., et al. 2007, A&A, 461, 813
- Chen, D.-M., & McGaugh, S. 2010, RAA (Research in Astronomy and Astrophysics), 10, 1215
- Chen, D.-M., & Zhao, H. 2006, ApJ, 650, L9
- Christensen, L., D'Odorico, S., Pettini, M., et al. 2010, MNRAS, 406, 2616
- Diehl, H. T., Allam, S. S., Annis, J., et al. 2009, ApJ, 707, 686
- Estrada, J., Annis, J., Diehl, H. T., et al. 2007, ApJ, 660, 1176

- Gladders, M. D., Hoekstra, H., Yee, H. K. C., Hall, P. B., & Barrientos, L. F. 2003, ApJ, 593, 48  
Hammer, F., & Rigaut, F. 1989, A&A, 226, 45  
Hennawi, J. F., Gladders, M. D., Oguri, M., et al. 2008, AJ, 135, 664  
Koester, B. P., Gladders, M. D., Hennawi, J. F., et al. 2010, ApJ, 723, L73  
Kubo, J. M., Allam, S. S., Annis, J., et al. 2009, ApJ, 696, L61  
Kubo, J. M., Allam, S. S., Drabek, E., et al. 2010, ApJ, 724, L137  
Li, G.-L., Mao, S., Jing, Y. P., et al. 2005, ApJ, 635, 795  
Li, N., & Chen, D. M. 2009, RAA (Research in Astronomy and Astrophysics), 9, 1173  
Limousin, M., Cabanac, R., Gavazzi, R., et al. 2009, A&A, 502, 445  
Lin, H., Buckley-Geer, E., Allam, S. S., et al. 2009, ApJ, 699, 1242  
Luppino, G. A., Gioia, I. M., Hammer, F., Le Fèvre, O., & Annis, J. A. 1999, A&AS, 136, 117  
Metcalfe, L., Kneib, J.-P., McBreen, B., et al. 2003, A&A, 407, 791  
Miralda-Escude, J., & Fort, B. 1993, ApJ, 417, L5  
Navarro, J. F., Frenk, C. S., & White, S. D. M. 1996, ApJ, 462, 563  
Ofek, E. O., Seitz, S., & Klein, F. 2008, MNRAS, 389, 311  
Pettini, M., Christensen, L., D'Odorico, S., et al. 2010, MNRAS, 402, 2335  
Sand, D. J., Treu, T., Ellis, R. S., & Smith, G. P. 2005, ApJ, 627, 32  
Schmidt, R. W., & Allen, S. W. 2007, MNRAS, 379, 209  
Shin, M.-S., Strauss, M. A., Oguri, M., et al. 2008, AJ, 136, 44  
Shu, C., Zhou, B., Bartelmann, M., et al. 2008, ApJ, 685, 70  
Stoughton, C., Lupton, R. H., Bernardi, M., et al. 2002, AJ, 123, 485  
Swinbank, A. M., Bower, R. G., Smith, G. P., et al. 2006, MNRAS, 368, 1631  
Takahashi, R., & Chiba, T. 2001, ApJ, 563, 489  
Wen, Z. L., Han, J. L., & Liu, F. S. 2009a, ApJS, 183, 197  
Wen, Z. L., Han, J. L., Xu, X. Y., et al. 2009b, RAA (Research in Astronomy and Astrophysics), 9, 5  
Wu, X.-P. 2000, MNRAS, 316, 299  
Wu, X.-P., & Mao, S. 1996, ApJ, 463, 404